FORUM GEOGRAFI
ISSN: 0852-0682 | E-ISSN: 2460-3945

HTTPS://JOURNALS.UMS.AC.ID/INDEX.PHP/FG/

Research article

Mapping of the Spatio-Spectral Dynamics of Mangrove Chlorophyll Concentrations via Sentinel-2 Satellite Imagery

K. K. Basheer Ahammed[1,2], I Wayan Gede Astawa Karang[1,*], I Wayan Nuarsa[1], I Gede Surya Indrawan[1], I Gede Hendrawan[1], Ni Made Nia Bunga Surya Dewi[3], Arvind Chandra Pandey[4]

[1] Department of Marine Science, Faculty of Marine Science and Fisheries, Udayana University, Jimbaran, Bali 80361 Indonesia
[2] International Union for the Conservation of Nature (IUCN), Commission on Ecosystem Management (CEM), South Asia
[3] Doctor of Environmental Science, Post Graduate Program, Udayana University, Jimbaran, Bali 80361 Indonesia
[4] Department of Geoinformatics, School of Natural Resource Management, Central University of Jharkhand, Cheri Manatu Rachi, 835 222 India

[*)] Correspondence: gedekarang@unud.ac.id

Citation:
Ahammed, B. K. K., Karang, I. W. G. A., Nuarsa, I. W., Indrawan, I. G. S., Dewi, N. M. N. B. S., & Pandey, A. C. (2024). Mapping of the Spatio-Spectral Dynamics of Mangrove Chlorophyll Con-centrations via Sentinel-2 Satellite Imagery. Forum Geografi. 38(2), 244-246.

Article history:
Received: 11 March 2024
Revised: 27 July 2024
Accepted: 28 July 2024
Published: 27 August 2024

Abstract

Mangrove ecosystems play a critical role in maintaining coastal health; however, they are increasingly threatened by anthropogenic activities and climate change. Health assessment is essential for effective conservation efforts. However, traditional remote sensing techniques such as the normalised difference vegetation index (NDVI) may not fully capture the complex physiological processes influencing vegetation health. Therefore, this study investigated chlorophyll (Chl) dynamics in mangroves using remote sensing techniques, including the NDVI and a novel method, the normalised area over reflectance curve (NAOC), via Sentinel-2 satellite imagery during October 2023, and analysed spatial variations in Chl content (CC) via the Google Earth Engine API. NDVI and NAOC-Chl were weakly correlated (0.47), highlighting their complementary roles. The average NDVI and NOAC-Chl values for different species were analysed, and Rhizophora mucronata presented the highest value (NDVI: 0.86 ± 0.08, NOAC: 20.48 ± 4.49 $\mu g/cm2$), whereas Sonneratia alba presented the lowest average CC (NDVI: 0.73 ± 0.07, NOAC: 13.45 ± 3.02 $\mu g/cm2$). The study also revealed spatial variations in CC, with potential stress near urban and water body areas and healthier vegetation in core than in the other regions. The disparities between northern and southern China suggest the impacts of human activity and climate change. We observed potential negative effects of unregulated tourism. This study provides insights for informed conservation strategies by demonstrating the value of combining remote sensing techniques and highlighting the importance of sustainable tourism practices.

Keywords: Google Earth Engine; Sentinel 2; Mangroves; Canopy chlorophyll; Vegetation health.

1. Introduction

The global mangrove ecosystem spans approximately 13.7 million hectares across 118 countries (Pastor-Guzman *et al.*, 2015; Wang *et al.*, 2023), whereas in Southeast Asia, mangroves extend over 4,000,000 ha and constitute 32.2% of the global mangrove area (Fauzi *et al.*, 2019). Mangrove forests serve as indispensable ecosystems, offering a plethora of direct and indirect services, such as acting as natural protection barriers and nursery habitats for marine organisms (Barbier & Strand, 1998; Ewel *et al.*, 1998; Pastor-Guzman *et al.*, 2015). The potential of mangroves as carbon sinks has garnered increasing attention recently, with estimates suggesting that mangrove carbon storage ranges from ~160 to ~1,000 Mg·ha−1, contingent upon factors such as location, species composition, height, and canopy closure (Lagomasino *et al.*, 2019; Matsui, 1998; Pastor-Guzman *et al.*, 2015). Despite their ecological importance and role in climate change mitigation, mangroves face significant threats including deforestation and land-use conversion (Akram *et al.*, 2023; Arifanti *et al.*, 2021).

Climate change has become the focus of discussions surrounding the fate of mangrove ecosystems as a combination of factors, including escalating temperatures, rising sea levels, greenhouse gas concentrations, shifts in ocean circulation and precipitation patterns, and an increase in extreme weather events, exert considerable pressure on these coastal habitats (Akram *et al.*, 2023; Alongi, 2022). The responses of mangroves to these environmental challenges hinge on the pivotal question of whether critical thresholds have been breached (Saenger *et al.*, 1983).

The productivity and carbon uptake of mangroves are closely related to photosynthesis, a process that depends on the availability of leaf pigments, with chlorophyll (Chl) being the main pigment (De *et al.*, 2021; Grove, 2017). Variations in leaf pigments serve as indicators of physiological status, senescence, and stress, and mangroves display pigment differences among species and health conditions (Hati *et al.*, 2021; Ku *et al.*, 2023; Pineda & Barón, 2022). Given their sensitivity to environmental gradients, particularly those induced by seasonal variations, such as water availability, understanding the Chl content (CC) is crucial for monitoring mangrove health and productivity (Cavalcanti *et al.*, 2022; Minu *et al.*, 2020; Wang & Gu, 2021).

Because of their unique adaptation to coastal environments, mangroves are exposed to an array of stressors induced by climate change (Kumari & Rathore, 2021). Elevated temperatures not only directly impact mangrove physiology but also influence sea levels through thermal expansion and the melting of polar ice, leading to altered inundation patterns (Beck Eichler & Barker, 2020; Çelekli & Zariç, 2023; Röthig *et al.*, 2023). Changes in precipitation patterns and ocean circulation further contribute to shifts in salinity levels, potentially exceeding the tolerance limits for mangrove species (de Lacerda *et al.*, 2022; Perri *et al.*, 2023).

Anthropogenic pressure driven by urbanisation and industrialisation, alongside land use change for agriculture and aquaculture, as well as the impact of tourism, collectively pose severe threats to the health of mangrove ecosystems (Basheer Ahammed & Pandey, 2021; Kumar *et al.*, 2022; Moorhouse *et al.*, 2021; Numbere, 2021; Umprasoet *et al.*, 2023). Pollution from industrial discharges, habitat destruction, and alterations in hydrological regimes disrupt the delicate balance of these coastal habitats. The conversion of mangrove areas to shrimp and fishponds contributes to habitat loss and fragmentation, and reduces resilience (Ballut-Dajud *et al.*, 2022; Chakraborty, 2019; Steven *et al.*, 2020). Unregulated tourism exacerbates this issue through habitat disturbance and pollution (Chandel, 2022). Mitigating these challenges requires integrated coastal zone management, community engagement, strengthened regulations, and educational efforts to strike a balance between the development and preservation of critical ecosystems.

CC estimation involves labour-intensive laboratory methods, including leaf pigment extraction and spectrophotometric determination (Croft *et al.*, 2015; Croft & Chen, 2017; Pastor-Guzman *et al.*, 2015). Portable Chl metres, such as SPAD and Apogee metres, offer a more practical alternative and have been successfully employed in precision agriculture in comparison to the lab measurement (Kamarianakis & Panagiotakis, 2023; Musacchi *et al.*, 2023; Odabas *et al.*, 2017). In the context of mangroves, the use of portable Chl metres has shown promise, as it provides correlations between CCs and metre readings. However, calibration equations are required to convert these readings to CCs (Dou *et al.*, 2018; Jiang *et al.*, 2008; Li *et al.*, 2023; Neres *et al.*, 2020).

Remote sensing has emerged as a powerful tool for estimating the CC, offering radiative transfer models and vegetation indices (VIs) (Ahmad *et al.*, 2020; Carmona *et al.*, 2015; Dou *et al.*, 2018; Liang *et al.*, 2016). Although radiative transfer models require computational resources, VIs represent a computationally simpler and accurate approach. VIs derived from hyperspectral and multispectral data have been applied to estimate vegetation CC in various settings. However, their application in mangrove forests remains relatively understudied (Connelly, 1997; Flores-de-Santiago *et al.*, 2013b, 2013a). This study sought to bridge this gap by assessing the performance of selected broadband VIs in predicting CC at the canopy level. Furthermore, it aimed to establish a link between the CCs of different species on the ground and Sentinel-2 (S2) data, paving the way for mapping the spatial distribution and variability of mangrove CCs at the landscape level. S2 strikes a good balance between high spatial resolution, multispectral capabilities, free access, and revisit frequency (Sentinel 2021), making it a valuable tool for studying Chl dynamics in mangroves. This study not only contributes to our understanding of mangrove ecosystems but also introduces the potential use of S2 data in mapping CCs, presenting valuable advancements in mangrove research.

Mangrove ecosystems are critical for coastal health; however, anthropogenic activities and climate change threaten their well-being. Traditional methods for assessing mangrove health do not provide a comprehensive picture, particularly at the species level. The present study addresses this gap by developing a method to invert canopy CCs in mangroves using high-resolution multispectral S2 satellite data. We employed both the established normalised difference vegetation index (NDVI) and novel normalised area over reflectance curve (NOAC) index. Although NDVI is widely used for vegetation monitoring, NOAC have undergone limited exploration, particularly in the context of mangroves. This research aimed not only to enhance our understanding of mangrove health but also to provide practical guidance for future monitoring and conservation efforts in the Tahura Ngurah Rai mangrove area (Benoa Bay) in Bali, Indonesia.

2. Materials and methods

2.1. Study area

The present study was carried out in the Tahura Ngurah Rai mangrove area (Benoa Bay), located in the Kuta and South Kuta Districts, Badung Regency, and Serangan Island, South Denpasar District, Denpasar City of Bali, Indonesia, with coordinates 08°41′–08°47′ South Latitude and 115°10′–115°15′ East Latitude (Figure 1). Bali has distinct tropical, wet, and dry climates. The wet season (November–April) is characterised by monsoon rains, with an average monthly rainfall of 341.62 mm in January. Conversely, the dry season (May–October) is cooler and less humid,

with average monthly rainfall dropping to a minimum of 39.93 mm in August. The annual average rainfall is 234–287 mm. Bali's topography is dominated by Gunung Agung, a 3,148 m stratovolcano, and the island's total coastline stretches for approximately 530 km, encompassing diverse features. Coastal areas include mangroves, beaches, and cliffs.

Bali, renowned for its vibrant tourism industry, faces significant challenges in the preservation of mangroves and other shallow-water ecosystems, resulting in the loss and deterioration of their health (Mahasani *et al.*, 2015; Sugiana *et al.*, 2022; Karang *et al.*, 2024). Mangrove areas are particularly vulnerable to these changes and experience direct impacts from land reclamation on tourist infrastructure and associated pollution from increased human activities (Newton *et al.*, 2020; Steven *et al.*, 2020). Coastal development can disrupt the natural hydrological patterns and affect the balance between salinity and water flow, which is crucial for mangrove health (Montagna *et al.*, 2012; Newton *et al.*, 2020; White & Kaplan, 2017).

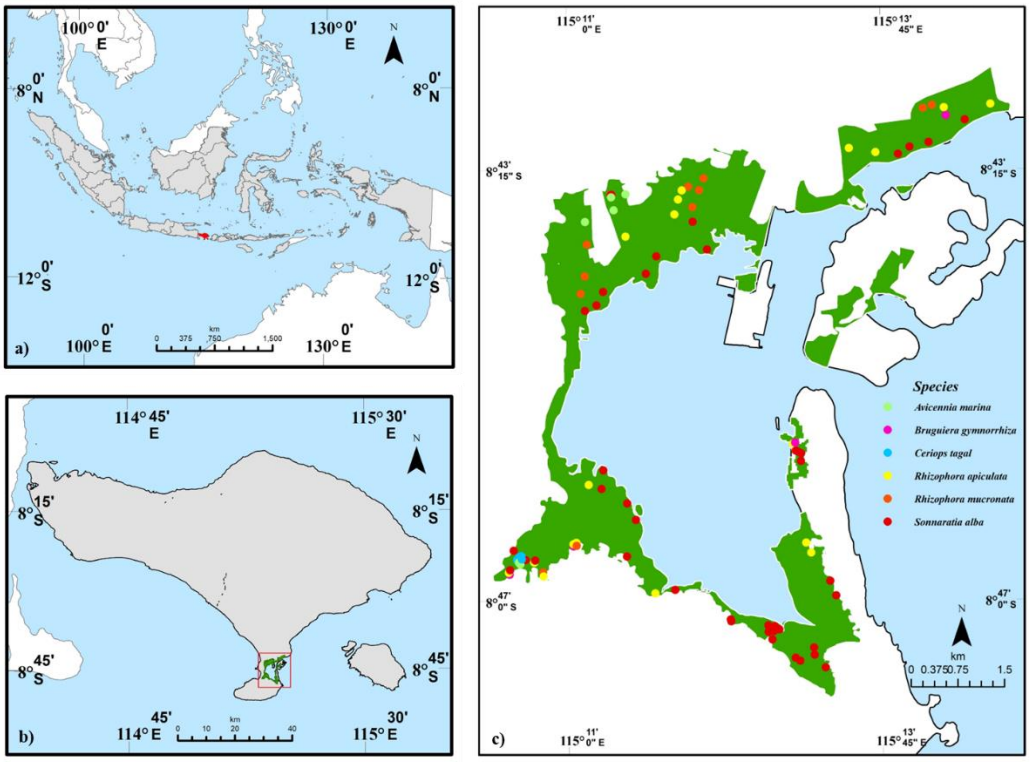

Figure 1. Location map of the study area: a) administrative area of Indonesia. b) Administrative area of Bali Province. c) Study area showing the locations of mangrove sample sites with dominant species.

2.2. Data acquisition

To determine the leaf canopy CC in various mangrove species, multiple field sampling surveys were conducted between October and November, 2023. The Global Positioning System (GPS) locations of the centre points from the 10 × 10 m field plots and the most dominant tree species in the field plot corresponding to the GPS location were collected (Figure 1). The sample points were strategically selected based on the accessibility and diversity of the species and were equally distributed across the study area. These sampling points were used for canopy CC mapping. This study focused on six mangrove stand types: Avicennia marina, Bruguiera gymnorrhiza, Ceriops tagal, Rhizophora apiculata, Rhizophora mucronata, and Sonneratia alba. S2 imagery with a resolution of 10 m guided the selection of 89 plots that were strategically positioned to encompass extensive patches dominated by individual species. This approach was followed to ensure the acquisition of pure pixels, each representing a distinct mangrove species.

2.3. Image acquisition and processing

S2 provides 13 spectral bands with varying spatial resolutions of 10–60 m (Table 1) and three red-edge bands (670–760 nm), which have proven successful in retrieving vegetation parameters. In this study, cloudless S2 level-2A surface reflectance products with radiometric and geometric corrections were acquired and processed via the Google Earth engine API, and their acquisition times ranged from 01–10–2023 to 20–11–2023 as the fieldwork was conducted between October and November. Twenty cloud-free images were acquired during this period. The means of all

available images were selected for further analysis. Averaging filters can help reduce noise and potentially improve the accuracy of CC estimates, particularly in areas with low inherent spatial variability (Xue *et al.*, 2023). All bands were resampled to a 10 m spatial resolution. Furthermore, 10 m spatial resolution bands were utilised for further analysis (Figure 2).

Table 1. General description of the Sentinel 2A and 2B satellite images.

Band name	Pixel size (m)	Wavelength S2A/S2B (mm)	Description
B1	60	443.9/442.3	Aerosols
B2	10	496.6/492.1	Blue
B3	10	560/559	Green
B4	10	664.5/665	Red
B5	20	703.9/703.8	Red edge 1
B6	20	740.2/739.1	Red edge 2
B7	20	782.5/779.7	Red edge 3
B8	10	835.1/833	NIR
B8A	20	864.8/864	Red edge 4
B9	60	945/943.2	Water vapour
B11	20	1,613.7/1,610.4	SWIR 1
B12	20	2,202.4/2,185.7	SWIR 2

2.4. Estimating canopy Chl value with VIs

VIs are crucial tools for estimating CC and leaf area index (LAI) in scientific research (Broge & Leblanc, 2001; Haboudane *et al.*, 2002; Liang *et al.*, 2016; Sun *et al.*, 2019). These indices simplify complex multispectral data and convert them into single variables for predicting and assessing various vegetation characteristics (Sun *et al.*, 2019). Among these indices, the NDVI (Weier & Herring, 2000) is a widely recognised and commonly employed metric.

The NDVI is calculated using Equation 1.

$$NDVI = \frac{\rho_{833} - \rho_{665}}{\rho_{833} + \rho_{665}} \quad (1)$$

Here, ρ_i represents the reflectance at the band centred at a specific wavelength i (in nm). CC, green biomass, nitrogen content, and LAI have been widely proven useful in diverse studies on plant development (Fava et *al.*, 2009; Pu *et al.*, 2008). In addition, numerous alternative indices sensitive to LAI have been proposed, often utilising bands in the red-edge regions (Daughtry *et al.*, 2000; Glenn *et al.*, 2008; Haboudane *et al.*, 2002). The typical spectra of vegetation present a plateau above 750–800 nm, which is determined by the structure and composition of leaves (Asner *et al.*, 1998); the soil response, excluding the Chl, is relatively featureless. The influence of Chl induces a minimum reflectance at approximately 665 nm, such that greater the presence of Chl. To estimate the amount of Chl in plants from multispectral data, the normalised area over the reflectance curve (NAOC) yields the best results among the other VIs, and thus, the NOAC was employed (Delegido *et al.*, 2010). Because S2 had many (narrow) bands available, it was possible to derive vegetation characteristics using a more continuous approach instead of using only two bands. Notably, certain characteristics of the S2 instrument, such as spatial size and signal-to-noise ratio, were not explicitly considered in the analysis. The S2 band configuration features three spectral bands situated in the red-edge region: bands B5 and B6 are positioned at the sharp edge, and band B7 is situated at the shoulder of the near-infrared (NIR) plateau. Importantly, these three bands, along with the B4 band, were aligned precisely within the integration limits of NAOC. The NAOC index was used to estimate the CC and was defined as described previously (Delegido *et al.*, 2010). Using the available bands in S2, the NAOC for estimating the CC was obtained with integration limits from a = 665 nm to b = 783 nm, resulting in a final expression for NAOC given by Equation 2.

$$NAOC = 1 - \frac{\int_{665}^{779} \rho \, d\lambda}{118 \quad \rho_{783}} \quad (2)$$

Furthermore, the CC estimated using NAOC can be expressed as follows (Equation 3).

$$Chl\ (\mu g/cm^2) = -3.8868 + 101.94 * NAOC \quad (3)$$

The NAOC has demonstrated its reliability as a predictor of Chl. In a recent study that compared its predictive efficacy against 32 established indices sensitive to Chl, NAOC was one of the best

performers, securing a position within the top three indices in terms of accuracy (Verrelst *et al.*, 2011).

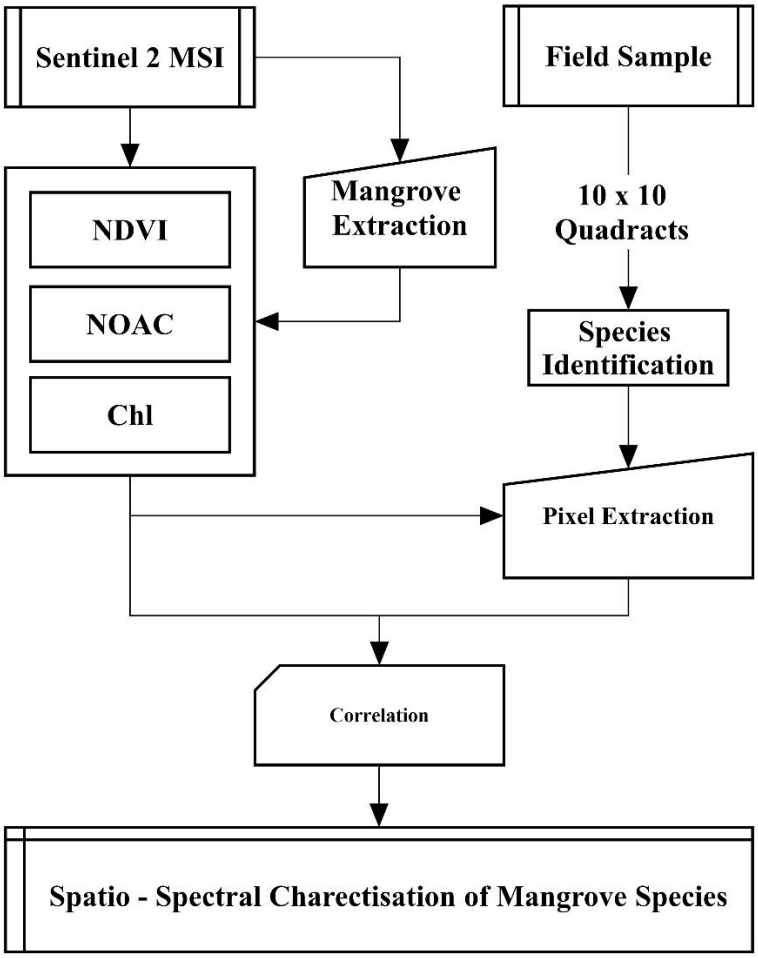

Figure 2. Schematic representation of the methodology workflow.

3. Results and Discussion

3.1. Spatial variation in CC

The assessment of leaf CC via S2 imagery has emerged as a pivotal element in understanding the intricate dynamics of vegetation health and ecological processes within the studied mangrove ecosystems. The observed NOAC-Chl ranged from 33.64 to 0 (Figure 3a), signifying a comprehensive depiction of vegetation conditions, with lower values coinciding with areas devoid of vegetation. The calculated average CC of 2.34 ± 8.92 provides a baseline metric for evaluating the overall Chl abundance in the study area. The observed NDVI values ranged between −0.66 and 0.97 (Figure 3b).

The spatial distribution of CC offers intriguing insights into the ecological dynamics of the mangrove landscape. The lowest CC in areas adjacent to water bodies and built-up structures suggested the presence of potential stressors in these regions (Figure 4). Vegetation in such areas is more stressed than that in other areas due to pollutants in the air and soil (Czaja *et al.*, 2020; Kannankai *et al.*, 2022; Zhao *et al.*, 2024). Conversely, the observation of the highest CC in the core areas of the mangrove patches indicates robust and healthy vegetation in these central regions owing to the absence of pollutants (Hai *et al.*, 2021). This spatial heterogeneity in CC reveals the potential impacts of urbanisation and proximity to water bodies on the Chl dynamics of mangrove ecosystems (Wong *et al.*, 2021; Zhao *et al.*, 2024).

Notably, a distinct pattern was observed, with high-Chl patches predominantly located in the northern part of the study area, whereas areas in the southern part of the study area presented signs of stress. This spatial variation may be attributed to a combination of factors, including developmental activities, waste disposal, and the influence of climate change scenarios such as rising temperatures and salinity (Arifanti 2020; Ng & Ong 2021). The suggestion of stress in the

southern areas necessitates further investigation to unravel the intricate interplay between anthropogenic and environmental factors influencing mangrove health.

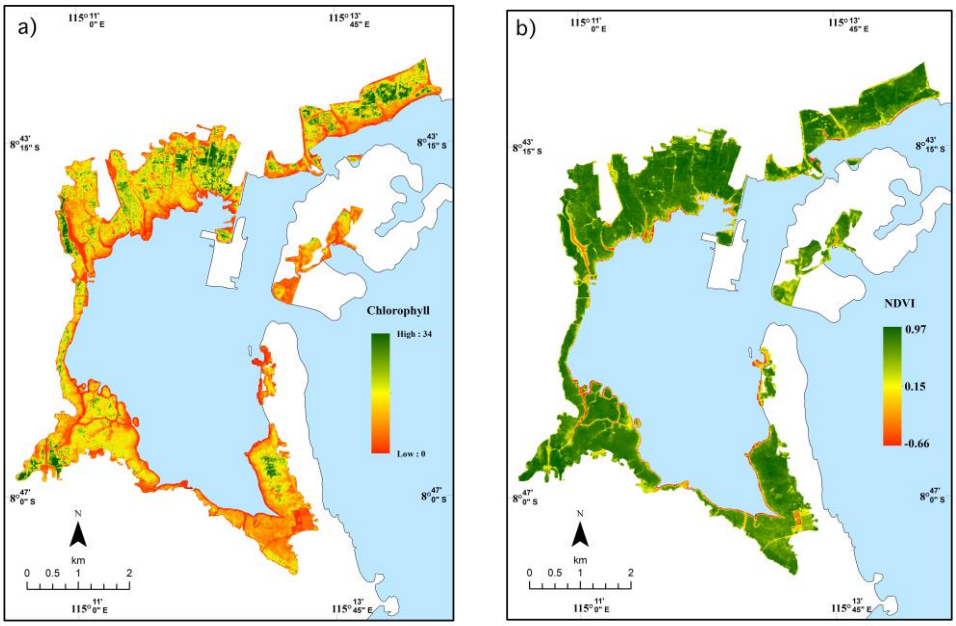

Figure 3. Maps showing the spatial variation in mangrove health derived from vegetation indices: a) NDVI and b) NOAC-Chl. ($\mu g/cm^2$).

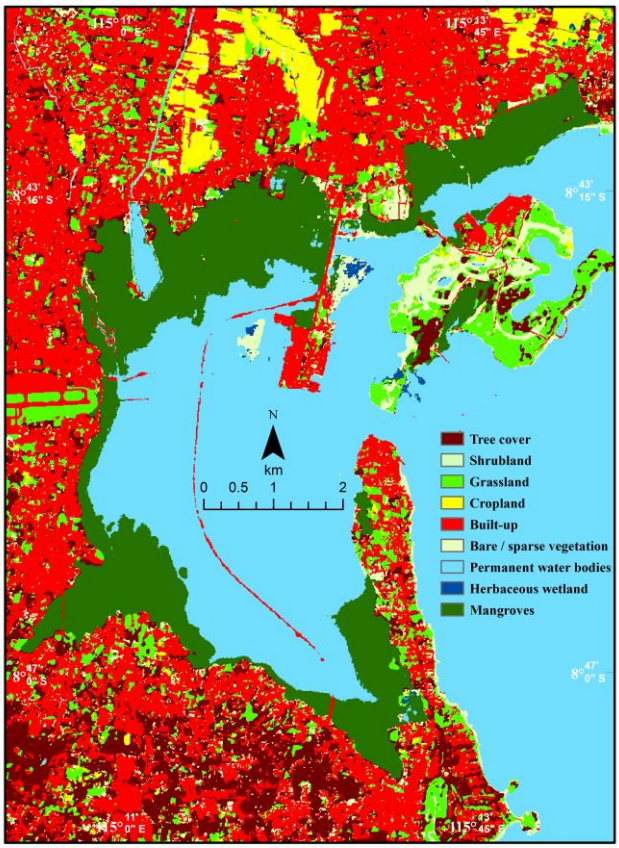

Figure 4. Land use/landcover map of the study area.

These findings highlight the utility of S2 in providing detailed insights into the spatial distribution of Chl, thereby enabling the identification of areas under potential stress and those exhibiting healthier vegetation conditions (Misra *et al.*, 2020). This knowledge is crucial for targeted conservation and management strategies, especially in urbanised and water-body-adjacent regions

where mangroves face heightened challenges (Czaja *et al.*, 2020; Kannankai *et al.*, 2022; Zhao *et al.*, 2024). Future analyses should delve deeper into the specific drivers of stress and their implications for mangrove resilience to offer a foundation for informed decision-making and sustainable management practices in the face of evolving environmental dynamics.

3.2. Canopy CC in mangrove species

The results obtained from the estimation of the CC in mangrove plant canopies using S2 imagery provide valuable insights into the ecological dynamics of different mangrove species. The application of the NDVI revealed distinct variations in vegetation density and health among the studied species (Rugel *et al.*, 2017). Ceriops tagal had the highest NDVI (0.94), indicating robust health, whereas R. apiculate presented the lowest NDVI (0.31), suggesting potential variations in vitality. The observed NDVI range (0.3–0.94) (Table 2) emphasised the diverse physiological conditions across the mangrove ecosystem.

Notably, the highest average NDVI values were associated with R. mucronata (0.86 ± 0.07), underscoring its elevated CC. Conversely, S. alba presented the lowest average NDVI (0.73 ± 0.08), suggesting potential differences in its CC. R. apiculata showed the greatest variation in the NDVI-based CC, highlighting its heterogeneous health conditions.

The introduction of the NAOC as a novel index for CC estimation further enriches this study. The CC variation induced by the NOAC reinforced the diversity in CC among the studied species (Figure 5, Table 3). R. mucronata presented the highest average CC (20.48 ± 4.49 $\mu g/cm2$), confirming its robust CC, whereas S. alba presented the lowest average CC (13.45 ± 3.02 $\mu g/cm^2$). A. marina presented the highest CC value (28.98 $\mu g/cm^2$), indicating its distinct Chl richness, whereas R. apiculata presented the lowest CC value (6.42 $\mu g/cm^2$) (Table 3).

These findings highlight the intricate interplay among species-specific CC in mangrove ecosystems. The observed variations underscore the importance of employing advanced remote sensing techniques, such as NDVI and NAOC, to capture nuanced ecological dynamics (Gafurov *et al.*, 2024; Su *et al.*, 2024). This study not only contributes to the understanding of mangrove health but also provides a foundation for future ecological assessments and conservation strategies tailored to the specific needs of different mangrove species. It is crucial to consider diverse Chl patterns in mangroves to formulate effective conservation and management practices in the face of environmental challenges.

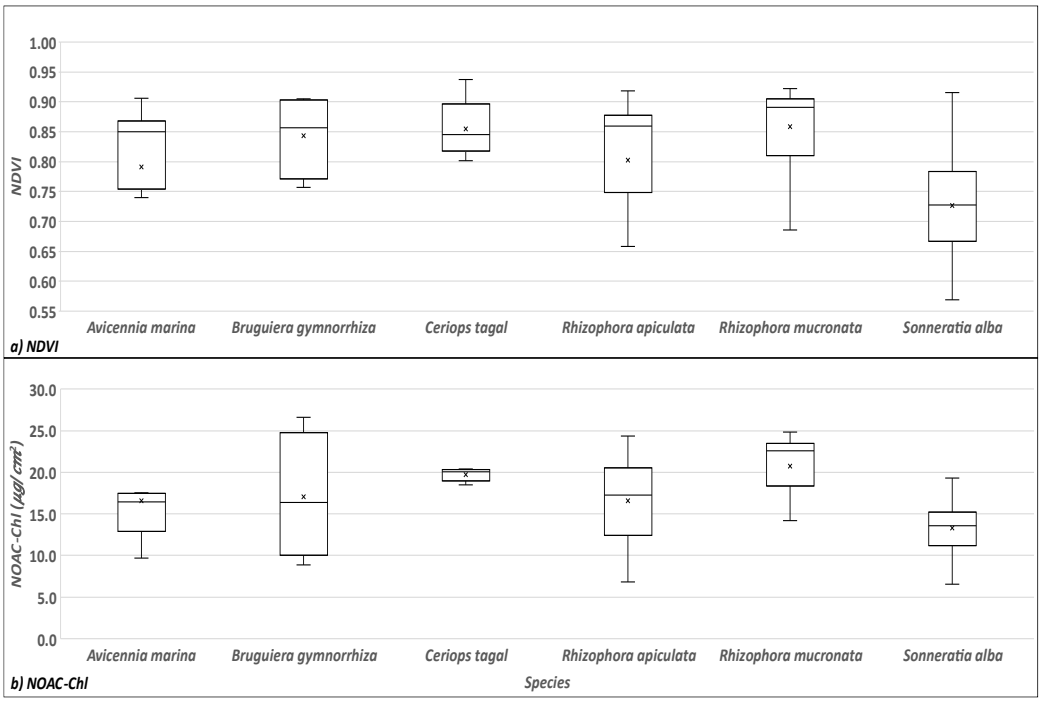

Figure 5. Chlorophyll concentrations in different species derived from a) the NDVI and b) NOAC-Chl. ($\mu g/cm2$). The box diagram shows the minimum and maximum values, and the black dots represent the average value of each species.

Table 2. Statistics of the NDVI values of different species.

Species	No of samples	Mean	Min	Max	SD
Avicennia marina	8	0.79	0.46	0.91	0.14
Bruguiera gymnorrhiza	4	0.84	0.76	0.90	0.07
Ceriops tagal	5	0.85	0.80	0.94	0.05
Rhizophora apiculata	18	0.80	0.31	0.92	0.14
Rhizophora mucronata	12	0.86	0.69	0.92	0.07
Sonneratia alba	42	0.73	0.57	0.92	0.08

Table 3. Statistics of NOAC-Chl values in different species.

Species	No of samples	Mean	Min	Max	SD
Avicennia marina	8	16.50	9.68	28.98	5.72
Bruguiera gymnorrhiza	4	17.08	8.87	26.06	7.36
Ceriops tagal	5	19.76	18.49	20.22	0.72
Rhizophora apiculata	18	16.17	6.42	24.33	5.47
Rhizophora mucronata	12	20.48	10.56	24.81	4.49
Sonneratia alba	42	13.45	6.52	19.13	3.02

3.3 Correlations between the NDVI and NOAC-Chl

The observed disparity in canopy CCs estimated via NDVI and NAOC prompted a meticulous exploration of their distinct sensitivities to vegetation health. The relatively low correlation coefficient ($r^2 \approx 0.43$) (Figure 6) between NDVI and NOAC-Chl suggests that these indices provide complementary information, each capturing unique aspects of Chl distribution in the studied mangrove ecosystem.

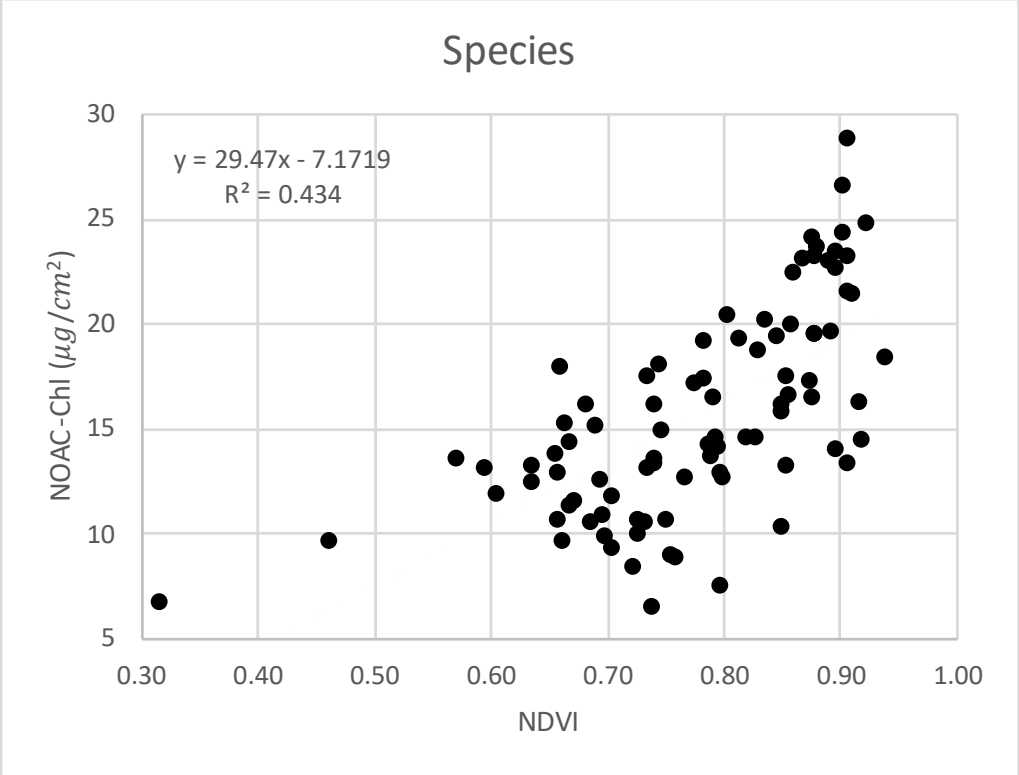

Figure 6. Scatter plot showing the correlation between the NDVI and NOAC-Chl.

The divergence in wavelength utilisation becomes evident in this study, with the NDVI relying on red and NIR bands and the NOAC incorporating multiple spectral bands in the red-edge region. This discrepancy in wavelength sensitivity contributed to the observed variation in CC. Owing to its broader spectral range, NDVI can capture different aspects of vegetation health, whereas NOAC, with its emphasis on red-edge bands, tends to offer a more refined perspective of Chl distribution (Cendrero *et al.*, 2014; Misra *et al.*, 2020; Sun *et al.*, 2023).

A comparative analysis revealed the superior performance of NOAC in Chl estimation compared to that of NDVI. This outcome aligns with the understanding that indices focusing on the red-edge region can provide more accurate assessments of CC than those focusing on the other regions, owing to their heightened sensitivity to subtle variations in leaf pigments and physiological conditions (Chang-Hua *et al.*, 2010; Cendrero *et al.*, 2014; Guimarães *et al.*, 2017).

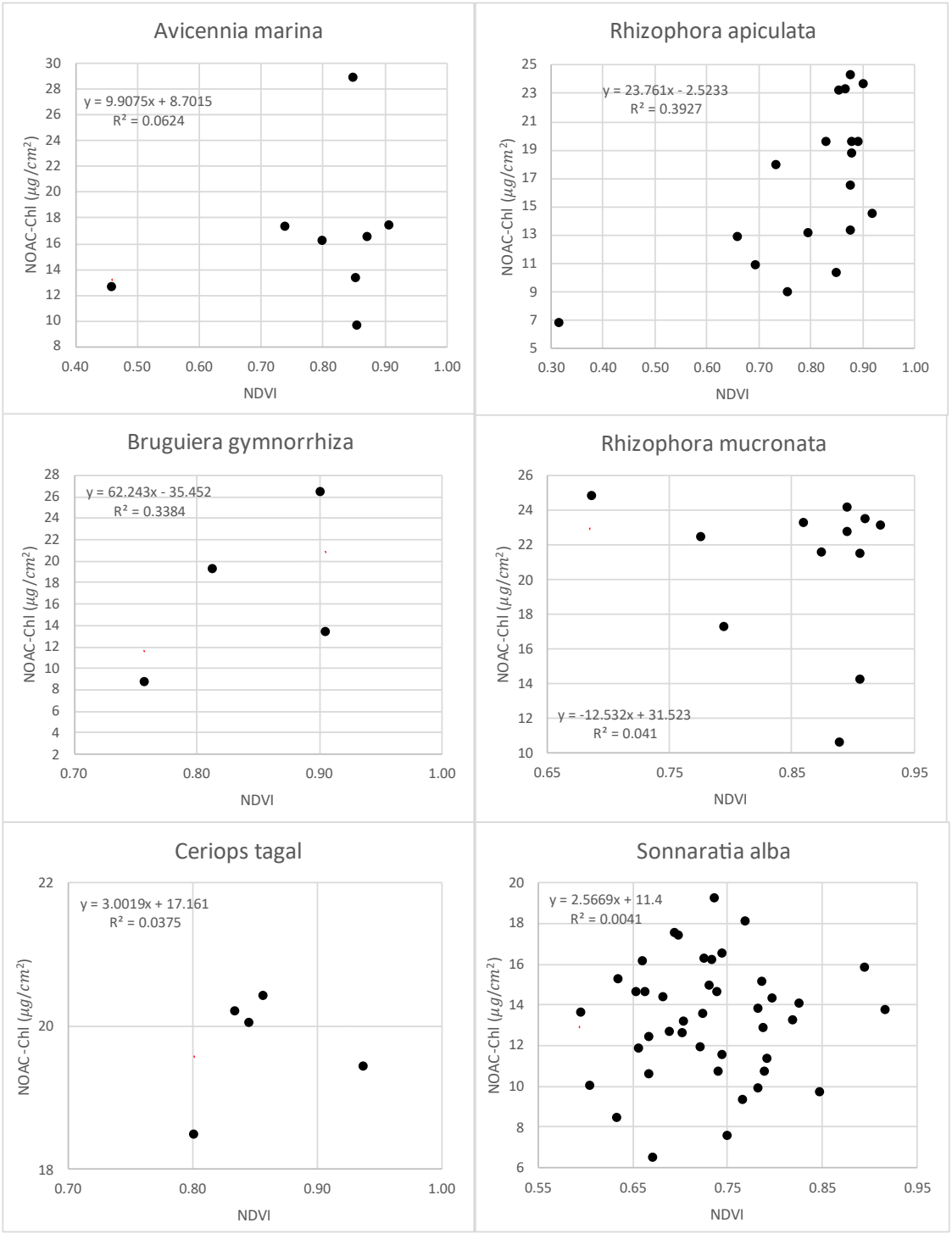

Figure 7. Scatter plots showing the correlation between the NDVI and NOAC-Chl. in different species.

Furthermore, species-specific correlation analyses provide insights on the subtle responses of different mangrove species to NDVI and NOAC. Notably, R. apiculata and B. gymnorhiza presented greater correlations in the two indices (r^2 = 0.39 and 0.33, respectively) (Figure 7), indicating a stronger alignment between the CCs of these species, as estimated by the NDVI and NOAC. In contrast, S. alba displayed a notably lower correlation (r^2 = 0.004) (Figure 7), sugges

Acknowledgements

The authors would like to thank ESA for the Sentinel data, Google for GEE platform. Special thanks to the Udayana University for the Support. This work was supported by the UNISERF Project DIPA PNBP of Udayana University FY 2023 (B/775-235/UN14.4.A/PT.01.03/2023, dated 26 July 2023) funded by the Udayana University, Indonesia

Author Contributions

Conceptualisation: Basheer Ahammed, K. K., Karang, I. W. G. A.; **methodology**: Basheer Ahammed , K. K., Karang**,** I. W. G. A., Nuarsa, I. W., Hendrawan, I. G., & Pandey, A. C.; **investigation**: Basheer Ahammed, K. K., Karang, I. W. G. A., Indrawan, I. G. S., & Dewi, N. M. N. B. S.; **writing—original draft preparation**: Basheer Ahammed, K. K., & Karang, I. W. G. A.; **writing—review and editing**: Basheer Ahammed, K. K., & Karang, I. W. G. A.; **visualisation**: Basheer Ahammed, K. K., & Karang, I. W. G. A. All authors have read and agreed to the published version of the manuscript.

Conflict of interest

All authors declare that they have no conflicts of interest.

Data availability

Data is available upon request.

Funding

This work was supported by the UNISERF Project DIPA PNBP of Udayana University FY 2023, inaccordance with the Research Implementation Assignement Letter (SP3) Number: B/775-235/UN14.4.A/PT.01.03/2023, dated 26 July 2023 funded by the Udayana University, Indonesia.

ting a potential divergence in the response of this species to the two indices. R. mucronata presented a unique

scenario with a negative correlation ($r^2 = -0.04$), necessitating further investigation into the underlying factors influencing Chl dynamics. The red-edge band is particularly valuable for identifying subtle variations in plant health and stress (Li *et al.*, 2024). As the CC decreases due to stress factors, such as nutrient deficiencies, diseases, or drought, the reflectance pattern in the red-edge region shifts (Chang-Hua *et al.*, 2010). The red-edge band can also be helpful in differentiating different vegetation types based on their CC and pigment composition. For example, healthy broadleaf plants typically exhibit steeper slopes in red-edge regions than do coniferous trees (Fernández *et al.*, 2022).

This study underscores the importance of selecting appropriate indices for accurate Chl estimation considering the unique spectral characteristics of different mangrove species. The dissimilarities between NDVI and NOAC highlight the need for a comprehensive approach that integrates multiple indices to capture the multifaceted nature of vegetation health in mangrove ecosystems. This fine understanding is crucial for developing informed conservation and management strategies tailored to the diverse physiological nuances of various mangrove species.

4. Conclusion

This study provides a comprehensive exploration of mangrove health and Chl dynamics in tropical ecosystems, using advanced remote sensing techniques. The integration of the NDVI and NAOC offers nuanced insights into Chl distribution among different mangrove species. The observed low correlation between NDVI and NOAC-Chl underscores the distinct scenarios captured by these indices, emphasising the importance of their complementary use for a comprehensive understanding of vegetation health.

Utilising S2 imagery, this study further enriches our understanding of CC, revealing spatial variations indicative of stressors and thriving vegetation patches within mangrove landscapes. The identification of lower Chl values near urban areas and water bodies, coupled with higher CCs in core mangrove regions, than those in the other areas implies the influence of anthropogenic activities on mangrove health. The spatial disparity between the northern and southern study areas suggests potential impacts of developmental activities, waste disposal, and climate change scenarios, emphasising the need for further investigation.

Moreover, this study addresses the broader context of anthropogenic pressures on mangrove health, specifically highlighting the detrimental impact of unregulated tourism practices. Boat traffic and recreational activities associated with tourism can cause physical damage to mangrove ecosystems, thereby contributing to the overall loss of mangrove areas and compromising their resilience. The cumulative effects of tourism-related pressures underscore the urgency of implementing sustainable tourism practices, stringent regulations, and community involvement. These measures are essential for mitigating the negative impacts and ensuring the preservation of Bali's mangrove ecosystems amid the flourishing tourism industry.

To summarise, this study not only advances our understanding of mangrove Chl dynamics but also underscores the critical need for integrated conservation strategies that consider the intricate interplay of environmental, anthropogenic, and tourism-related factors. By adopting a holistic approach informed by the findings of this study, we can pave the way for sustainable management and preservation of mangrove ecosystems in the face of ongoing environmental changes and human activities.

References

Ahmad, S., Pandey, A. C., Kumar, A., Parida, B. R., Lele, N. V., & Bhattacharya, B. K. (2020). Chlorophyll deficiency (chlorosis) detection based on spectral shift and yellowness index using hyperspectral AVIRIS-NG data in Sholayar reserve forest, Kerala. *Remote Sensing Applications: Society and Environment*, 19, 100369. doi: 10.1016/j.rsase.2020.100369

Akram, H., Hussain, S., Mazumdar, P., Chua, K. O., Butt, T. E., & Harikrishna, J. A. (2023). Mangrove Health: A Review of Functions, Threats, and Challenges Associated with Mangrove Management Practices. *Forests*, 14(9), 1698. doi: 10.3390/f14091698

Alongi, D. M. (2022). Climate Change and Mangroves. In S. C. Das, Pullaiah, & E. C. Ashton. (2022). Mangroves: Biodiversity, Livelihoods and Conservation. *Springer Nature Singapore*, 175–19. doi: 10.1007/978-981-19-0519-3_8

Arifanti, V. B. (2020). Mangrove management and climate change: a review in Indonesia. In IOP conference series: earth and environmental science. *IOP Publishing*, 487(1), 012022. doi: 10.1088/1755-1315/487/1/012022

Arifanti, V. B., Novita, N., & Tosiani, A. (2021). Mangrove deforestation and CO2 emissions in Indonesia. *IOP Conference Series: Earth and Environmental Science*, 874(1), 012006. doi: 10.1088/1755-1315/874/1/012006

Asner, G. P., Wessman, C. A., & Archer, S. (1998). Scale Dependence Of Absorption Of Photosynthetically Active Radiation In Terrestrial Ecosystems. *Ecological Applications*, 8(4), 1003–1021. doi: 10.1890/1051-0761(1998)008[1003:SDOAOP]2.0.CO;2

Ballut-Dajud, G. A., Sandoval Herazo, L. C., Fernández-Lambert, G., Marín-Muñiz, J. L., López Méndez, M. C., & Betanzo-Torres, E. A. (2022). Factors affecting wetland loss: A review. *Land*, 11(3), 434. doi: 10.3390/land11030434

Barbier, E. B., & Strand, I. (1998). Valuing mangrove-fishery linkages–a case study of Campeche, Mexico. *Environmental and Resource Economics*, 12(2), 151–166. doi: 10.1023/A:1008248003520

Basheer Ahammed, K. K., & Pandey, A. C. (2021). Characterization and impact assessment of super cyclonic storm AMPHAN in the Indian subcontinent through space borne observations. *Ocean & Coastal Management*, 205, 105532. doi: 10.1016/j.ocecoaman.2021.105532

Beck Eichler, P. P., & Barker, C. P. (2020). Sea Level Forecast Indicators: Sea-Level Rise Forecast by "The Moon and Sun" Foraminifera Species Indicators. In P. P. Beck Eichler & C. P. Barker, Benthic Foraminiferal Ecology. *Springer International Publishing*, 111–132. doi: 10.1007/978-3-030-61463-8_7

Broge, N. H., & Leblanc, E. (2001). Comparing prediction power and stability of broadband and hyperspectral vege-tation indices for estimation of green leaf area index and canopy chlorophyll density. *Remote Sensing of Envi-ronment*, 76(2), 156–172. doi: 10.1016/S0034-4257(00)00197-8

Carmona, F., Rivas, R., & Fonnegra, D. C. (2015). Vegetation Index to estimate chlorophyll content from multispectral remote sensing data. *European Journal of Remote Sensing*, 48(1), 319–326. doi: 10.5721/EuJRS20154818

Cavalcanti, L. F., do N Feitosa, F. A., Cutrim, M. V., de JF Montes, M., Lourenço, C. B., Furtado, J. A., & dos S Sá, A. K. D. (2022). Drivers of phytoplankton biomass and diversity in a macrotidal bay of the Amazon Mangrove Coast, a Ramsar site. *Ecohydrology & Hydrobiology*, 22(3), 435–453. doi: 10.1016/S0034-4257(00)00197-8

Çelekli, A., & Zariç, Ö. E. (2023). *Hydrobiology and ecology in the context of climate change: The future of aquatic ecosystems.* Retrieved from https://aperta.ulakbim.gov.tr/record/263238

Cendrero-Mateoa, M. P., Moranb, M. S., Papugaa, S. A., Laparrad, V., Ponce-Camposb, G., Riverad, J. P., & Wange, G. (2014). *Appendix C: Seasonal Variation Of Net Photosynthesis And Chlorophyll Fluorescence Under Nitrogen Treatments In Wheat*. Chlorophyll Fluorescence Response To Water And Nitrogen Deficit, 88.

Chakraborty, S. K. (2019). Bioinvasion and Environmental Perturbation: Synergistic Impact on Coastal–Mangrove Ecosystems of West Bengal, India. In C. Makowski & C. W. Finkl (Eds.), *Impacts of Invasive Species on Coas-tal Environments Springer International Publishing*, 29, 171–245. doi: 10.1007/978-3-319-91382-7_6

Chandel, S. P. K. (2022). Impacts of Tourism on Environment. *Central Asian Journal of Innovations on Tourism Management and Finance*, 3(10), 90–98.

Chang-Hua, J. U., Yong-Chao, T. I. A. N., Xia, Y. A. O., Wei-Xing, C. A. O., Yan, Z. H. U., & Hannaway, D. (2010). Es-timating leaf chlorophyll content using red edge parameters. *Pedosphere*, 20(5), 633-644. doi: 10.1016/S1002-0160(10)60053-7

Chang-Hua, J. U., Yong-Chao, T., Xia, Y. A. O., Wei-Xing, C. A. O., Yan, Z. H. U., & Hannaway, D. (2010). Estimating leaf chlorophyll content using red edge parameters. *Pedosphere*, 20(5), 633–644.

Connelly, X. M. (1997). *The Use of a chlorophyll meter (SPAD-502) for field determinations of red mangrove (Rhizophora Mangle L.) leaf chlorophyll amount. NASA University Research Centers Technical Advances in Education, Aeronautics, Space, Autonomy, Earth and Environment, 1(URC97032).* Retrieved from https://ntrs.nasa.gov/citations/20010000391

Croft, H., & Chen, J. M. (2017). Leaf pigment content. Comprehensive *Remote Sensing*, 3, 117–142.

Croft, H., Chen, J. M., Zhang, Y., Simic, A., Noland, T. L., Nesbitt, N., & Arabian, J. (2015). Evaluating leaf chlorophyll content prediction from multispectral remote sensing data within a physically based modelling framework. *ISPRS Journal of Photogrammetry and Remote Sensing*, 102, 85–95. doi: 10.1016/j.isprsjprs.2015.01.008

Czaja, M., Kołton, A., & Muras, P. (2020). The complex issue of urban trees—Stress factor accumulation and ecologi-cal service possibilities. *Forests*, 11(9), 932.

Daughtry, C. S., Walthall, C. L., Kim, M. S., De Colstoun, E. B., & McMurtrey Iii, J. E. (2000). Estimating corn leaf chlorophyll concentration from leaf and canopy reflectance. *Remote Sensing of Environment*, 74(2), 229–239. doi: 10.1016/S0034-4257(00)00113-9

de Lacerda, L. D., Ward, R. D., Borges, R., & Ferreira, A. C. (2022). Mangrove trace metal biogeochemistry response to global climate change. *Frontiers in Forests and Global Change*, 5, 47. doi: 10.3389/ffgc.2022.817992

De, T. K., Raman, M., Sarkar, S. K., & Mukherjee, A. (2021). Ecological assessment of Hooghly River considering a few of the more perturbed sites based on some relevant physico-chemical and biological variables—A part of the AVIRIS-NG (NASA-ISRO) ground truth verification. *Regional Studies in Marine Science*, 41, 101598.

Delegido, J., Alonso, L., Gonzalez, G., & Moreno, J. (2010). Estimating chlorophyll content of crops from hyperspectral data using a normalized area over reflectance curve (NAOC). *International Journal of Applied Earth Observation and Geoinformation*, 12(3), 165–174. doi: 10.1016/j.jag.2010.02.003

Dou, Z., Cui, L., Li, J., Zhu, Y., Gao, C., Pan, X., Lei, Y., Zhang, M., Zhao, X., & Li, W. (2018). Hyperspectral estimation of the chlorophyll content in short-term and long-term restorations of mangrove in Quanzhou Bay Estuary, China. *Sustainability*, 10(4), 1127. doi: 10.3390/su10041127

Ewel, K., Twilley, R., & Ong, J. I. N. (1998). Different kinds of mangrove forests provide different goods and services. *Global Ecology & Biogeography Letters*, 7(1), 83–94. doi: 10.1111/j.1466-8238.1998.00275.x

Fauzi, A., Sakti, A., Yayusman, L., Harto, A., Prasetyo, L., Irawan, B., Kamal, M., & Wikantika, K. (2019). Contextualizing mangrove forest deforestation in southeast asia using environmental and socioeconomic data products. *Forests*, 10(11), 952. doi: 10.3390/f10110952

Fava, F., Colombo, R., Bocchi, S., Meroni, M., Sitzia, M., Fois, N., & Zucca, C. (2009). Identification of hyperspectral vegetation indices for Mediterranean pasture characterization. *International Journal of Applied Earth Obser-vation and Geoinformation*, 11(4), 233–243. doi: 10.1016/j.jag.2009.02.003

Fernández-Tejedor, M., Velasco, J. E., & Angelats, E. (2022). Accurate estimation of Chlorophyll-a concentration in the coastal areas of the Ebro Delta (NW Mediterranean) using Sentinel-2 and its application in the selection of areas for mussel aquaculture. *Remote Sensing*, 14(20), 5235. doi: 10.3390/rs14205235

Flores-de-Santiago, F., Kovacs, J. M., & Flores-Verdugo, F. (2013a). Assessing the utility of a portable pocket instrument for estimating seasonal mangrove leaf chlorophyll contents. *Bulletin of Marine Science*, 89(2), 621–633. doi: 10.5343/bms.2012.1032

Flores-de-Santiago, F., Kovacs, J. M., & Flores-Verdugo, F. (2013b). The influence of seasonality in estimating mangrove leaf chlorophyll-a content from hyperspectral data. *Wetlands Ecology and Management*, 21(3), 193–207. doi: 10.1007/s11273-013-9290-x

Gafurov, A., Prokhorov, V., Kozhevnikova, M., & Usmanov, B. (2024). Forest Community Spatial Modelling Using Machine Learning and Remote Sensing Data. *Remote Sensing*, 16(8), 1371. doi: 10.3390/rs16081371

Glenn, E. P., Huete, A. R., Nagler, P. L., & Nelson, S. G. (2008). Relationship between remotely sensed vegetation indices, canopy attributes and plant physiological processes: What vegetation indices can and cannot tell us about the landscape. *Sensors*, 8(4), 2136–2160. doi: 10.3390/s8042136

Grove, D. (2021). *Ocean acidification and carbon limitation affect photosynthetic capacity of the seagrass (Amphibo-lis antarctica) and its calcifying epiphytes [PhD Thesis, University of Plymouth].* Retrieved from https://pearl.plymouth.ac.uk/handle/10026.1/17162

Guimarães, T. T., Veronez, M. R., Koste, E. C., Gonzaga Jr, L., Bordin, F., Inocencio, L. C., ... & Mauad, F. F. (2017). An alternative method of spatial autocorrelation for chlorophyll detection in water bodies using remote sensing. *Sustainability*, 9(3), 416. doi: 10.3390/su9030416

Haboudane, D., Miller, J. R., Tremblay, N., Zarco-Tejada, P. J., & Dextraze, L. (2002). Integrated narrow-band vegetation indices for prediction of crop chlorophyll content for application to precision agriculture. *Remote Sensing of Environment*, 81(2), 416–426. doi: 10.1016/S0034-4257(02)00018-4

Hai, P. M., Tinh, P. H., Son, N. P., Thuy, T. V., Hanh, N. T. H., Sharma, S., Hoai, D. T., & Duy, V. C. (2022). Mangrove health assessment using spatial metrics and multi-temporal remote sensing data. *Plos one*, 17(12), e0275928. doi: 10.1371/journal.pone.0275928

Hati, J. P., Goswami, S., Samanta, S., Pramanick, N., Majumdar, S. D., Chaube, N. R., Misra, A., & Hazra, S. (2021). Estimation of vegetation stress in the mangrove forest using AVIRIS-NG airborne hyperspectral data. *Modelling Earth Systems and Environment*, 7, 1877–1889.

Jiang, H., Halverson, J. B., & Simpson, J. (2008). On the differences in storm rainfall from Hurricanes Isidore and Lili. Part I: Satellite observations and rain potential. *Weather and Forecasting*, 23(1), 29–43. doi: 10.1175/2007WAF2005096.1

Kamarianakis, Z., & Panagiotakis, S. (2023). Design and Implementation of a Low-Cost Chlorophyll Content Meter. *Sensors*, 23(5), 2699. doi: 10.3390/s23052699

Kannankai, M. P., Alex, R. K., Muralidharan, V. V., Nazeerkhan, N. P., Radhakrishnan, A., & Devipriya, S. P. (2022). Urban mangrove ecosystems are under severe threat from microplastic pollution: a case study from Mangalavanam, Kerala, India. *Environmental Science and Pollution Research*, 29(53), 80568-80580.

Karang, I. W. G. A., Pravitha, N. L. P. R., Nuarsa, I. W., Basheer Ahammed K. K, & WicaksonoPramaditya. (2024). High-resolution seagrass species mapping and propeller scars detection in Tanjung Benoa, Bali through UAV imagery. *Journal of Ecological Engineering*, 25(1). doi: 10.12911/22998993/174943

Ku, K.-B., Mansoor, S., Han, G. D., Chung, Y. S., & Tuan, T. T. (2023). Identification of new cold tolerant Zoysia grass species using high-resolution RGB and multispectral imaging. *Scientific Reports*, 13(1), 13209.

Kumar, N., Deepak, P. M., Basheer Ahammed, K. K., Rao, K. N., Gopinath, G., & Dinesan, V. P. (2022). Coastal vulnerability assessment using Geospatial technologies and a Multi-Criteria Decision Making approach–a case study of Kozhikode District coast, Kerala State, India. *Journal of Coastal Conservation*, 26(3), 1–14.

Kumari, A., & Rathore, M. S. (2021). *Roles of Mangroves in Combating the Climate Change. In R. P. Rastogi, M. Phulwaria, & D. K. Gupta (Eds.), Mangroves: Ecology, Biodiversity and Management (pp. 225–255).* Retrieved from https://link.springer.com/chapter/10.1007/978-981-16-2494-0_10

Lagomasino, D., Fatoyinbo, T., Lee, S., Feliciano, E., Trettin, C., Shapiro, A., & Mangora, M. M. (2019). Measuring mangrove carbon loss and gain in deltas. *Environmental Research Letters*, 14(2), 025002. doi: 10.1088/1748-9326/aaf0de

Li, H., Cui, L., Dou, Z., Wang, J., Zhai, X., Li, J., Zhao, X., Lei, Y., Wang, J., & Li, W. (2023). Hyperspectral Analysis and Regression Modelling of SPAD Measurements in Leaves of Three Mangrove Species. *Forests*, 14(8), 1566. doi: 10.3390/f14081566

Li, N., Huo, L., & Zhang, X. (2024). Using only the red-edge bands is sufficient to detect tree stress: A case study on the early detection of PWD using hyperspectral drone images. *Computers and Electronics in Agriculture*, 217, 108665. doi: 10.1016/j.compag.2024.108665

Liang, L., Qin, Z., Zhao, S., Di, L., Zhang, C., Deng, M., Lin, H., Zhang, L., Wang, L., & Liu, Z. (2016). Estimating crop chlorophyll content with hyperspectral vegetation indices and the hybrid inversion method. *International Journal of Remote Sensing*, 37(13), 2923–2949. doi: 10.1080/01431161.2016.1186850

Mahasani, I., Widagti, N., & Karang, I. (2015). Estimasi persentase karbon organik di hutan mangrove bekas tambak, Perancak, Jembrana, Bali. *Journal of Marine and Aquatic Sciences*, 1(1), 14–18.

Matsui, N. (1998). Estimated stocks of organic carbon in mangrove roots and sediments in Hinchinbrook Channel, Australia. *Mangroves and Salt Marshes*, 2, 199–204.

Minu, A., Routh, J., Machiwa, J., & Pamba, S. (2020). Spatial variation of nutrients and primary productivity in the Rufiji Delta mangroves, Tanzania. *African Journal of Marine Science*, 42(2), 221–232. doi:10.2989/1814232X.2020.1776391

Misra, G., Cawkwell, F., & Wingler, A. (2020). Status of phenological research using Sentinel-2 data: A review. *Remote Sensing*, 12(17), 2760.

Misra, G., Cawkwell, F., & Wingler, A. (2020). Status of phenological research using Sentinel-2 data: A review. *Remote Sensing*, 12(17), 2760. doi: 10.3390/rs12172760

Montagna, P., Palmer, T. A., & Pollack, J. B. (2012). *Hydrological changes and estuarine dynamics (Vol. 8). Springer Science & Business Media.* Retrived from https://books.google.co.in/books?hl=en&lr=&id=7hymBy82V5EC&oi=fnd&pg=PR3&dq=Coastal+developments+can+disrupt+natural+hydrological+patterns,+affecting+the+intrcate+balance+of+salinity+and+water+flow+crucial+for+mangrove+health.+&ots=dDoWiB6O&sig=4ao9yifjdgFJX0TCKz3aBBH0wFE#v=onepage&q&f=false

Moorhouse, H. L., Roberts, L. R., McGowan, S., Panizzo, V. N., Barker, P., Salehin, M., Do, T. N., Nguyen Thanh, P., Rahman, M. F., Ghosh, T., Das, S., Hackney, C., Salgado, J., Roy, M., Opel, A., Henderson, A. C. G., & Large, A. R. G. (2021). Tropical Asian mega-delta ponds: Important and threatened socio-ecological systems. *Geo: Geography and Environment*, 8(2), e00103. doi:10.1002/geo2.103

Musacchi, S., Sheick, R., Mia, M. J., & Serra, S. (2023). Studies on physiological and productive effects of multileader training systems and Prohexadione-Ca applications on apple cultivar'WA 38′. *Scientia Horticulturae*, 312, 111850.

Neres, J., Dodonov, P., Mielke, M. S., & Strenzel, G. M. R. (2020). *Relationships between portable chlorophyll meter estimates for the red mangrove tree (Rhizophora mangle L.). Ocean and Coastal Research, 68*. Retrieved from https://www.scielo.br/j/ocr/a/jyGNrw5BGcHwsLyjh3NSpSr/?lang=en

Newton, A., Icely, J., Cristina, S., Perillo, G. M., Turner, R. E., Ashan, D., Cragg, S., Luo, Y., Tu, C., & Li, Y. (2020). An-thropogenic, direct pressures on coastal wetlands. *Frontiers in Ecology and Evolution*, 8, 144.

Ng, C. K. C., & Ong, R. C. (2022). A review of anthropogenic interaction and impact characteristics of the Sundaic mangroves in Southeast Asia. *Estuarine, Coastal and Shelf Science*, 267, 107759.

Numbere, A. O. (2021). Impact of Urbanization and Crude Oil Exploration in Niger Delta Mangrove Ecosystem and Its Livelihood Opportunities: A Footprint Perspective. In A. Banerjee, R. S. Meena, M. K. Jhariya, & D. K. Yadav (Eds.), Agroecological Footprints Management for Sustainable Food System (pp. 309–344). *Springer Singa-pore*. doi: 10.1007/978-981-15-9496-0_10

Odabas, M. S., Senyer, N., Kayhan, G., & Ergun, E. (2017). Estimation of Chlorophyll Concentration Index at Leaves using Artificial Neural Networks. *Journal of Circuits, Systems and Computers*, 26(02), 1750026. doi: 10.1142/S0218126617500268

Pastor-Guzman, J., Atkinson, P. M., Dash, J., & Rioja-Nieto, R. (2015). Spatiotemporal variation in mangrove chlorophyll concentration using Landsat 8. *Remote Sensing*, 7(11), 14530–14558.

Perri, S., Detto, M., Porporato, A., & Molini, A. (2023). Salinity-induced limits to mangrove canopy height. *Global Ecology and Biogeography*, 32(9), 1561–1574. https://doi.org/10.1111/geb.13720

Pineda, M., & Barón, M. (2022). Health status of oilseed rape plants grown under potential future climatic conditions assessed by invasive and noninvasive techniques. *Agronomy*, 12(8), 1845.

Pu, R., Gong, P., Tian, Y., Miao, X., Carruthers, R. I., & Anderson, G. L. (2008). Using classification and NDVI differencing methods for monitoring sparse vegetation coverage: A case study of saltcedar in Nevada, USA. *International Journal of Remote Sensing*, 29(14), 3987–4011. doi: 10.1080/01431160801908095

Röthig, T., Trevathan-Tackett, S. M., Voolstra, C. R., Ross, C., Chaffron, S., Durack, P. J., Warmuth, L. M., & Sweet, M. (2023). Human-induced salinity changes impact marine organisms and ecosystems. *Global Change Biology*, 29(17), 4731–4749. doi: 10.1111/gcb.16859

Rugel, E. J., Henderson, S. B., Carpiano, R. M., & Brauer, M. (2017). Beyond the normalized difference vegetation index (NDVI): developing a natural space index for population-level health research. *Environmental research*, 159, 474-483.

Saenger, P., Hegerl, E. J., & Davie, J. D. (1983). *Global status of mangrove ecosystems. International Union for Conservation.* Nature and Natural Resources.

Sentinel, C. (2021). *2.:(processed by ESA), MSI Level-2A BOA Reflectance Product*. Collection 1.

Steven, A., Addo, K. A., Llewellyn, G., Ca, V. T., Boateng, I., Bustamante, R., Doropoulos, C., Gillies, C., Hemer, M., & Lopes, P. (2020). *Coastal development: Resilience, restoration and infrastructure requirements. World Resources Institute, Washington DC.* Retrieved from Www. Oceanpanel. Org/b l Ue-Papers/Coastal-Development-Resilience-Restoration-and-Infrastructure-Requi r Ements.

Su, Z., Shen, J., Sun, Y., Hu, R., Zhou, Q., & Yong, B. (2024). *Deep Spatio-Temporal Fuzzy Model for NDVI Forecasting. IEEE Transactions on Fuzzy Systems*. Retrieved from https://smujo.id/biodiv/article/view/11293

Sugiana, I. P., Andiani, A. A. E., Dewi, I. G. A. I. P., Karang, I. W. G. A., As-Syakur, A. R., & Dharmawan, I. W. E. (2022). Spatial distribution of mangrove health index on three genera dominated zones in Benoa Bay, Bali, Indonesia. *Biodiversitas Journal of Biological Diversity*, 23(7).

Sun, Y., Qin, Q., Ren, H., Zhang, T., & Chen, S. (2019). Red-edge band vegetation indices for leaf area index estimation from sentinel-2/msi imagery. *IEEE Transactions on Geoscience and Remote Sensing*, 58(2), 826–840.

Sun, Y., Wang, B., & Zhang, Z. (2023). Improving leaf area index estimation with chlorophyll insensitive multispectral red-edge vegetation indices. *IEEE Journal of Selected Topics in Applied Earth Observations and Remote Sensing*, 16, 3568-3582. doi: 10.1109/JSTARS.2023.3262643

Umprasoet, W., Mu, Y., Somrup, S., Junchompoo, C., Guo, Z., & Zhang, Z. (2023). Assessment of Habitat Risks Caused by Human Activities and Integrated Approach to Marine Spatial Planning: The Case of Sriracha District—Sichang Island. *Coasts*, 3(3), 190–208.

Verrelst, J., Alonso, L., Camps-Valls, G., Delegido, J., & Moreno, J. (2011). Retrieval of vegetation biophysical parameters using Gaussian process techniques. *IEEE Transactions on Geoscience and Remote Sensing*, 50(5), 1832–1843. doi: 10.1109/TGRS.2011.2168962

Wang, F., Liu, J., Qin, G., Zhang, J., Zhou, J., Wu, J., ... & Ren, H. (2023). Coastal blue carbon in China as a nature-based solution towards carbon neutrality. The Innovation, 4(5), 100481. doi: 10.1016/j.xinn.2023.100481

Wang, Y.-S., & Gu, J.-D. (2021). Ecological responses, adaptation and mechanisms of mangrove wetland ecosystem to global climate change and anthropogenic activities. *International Biodeterioration & Biodegradation*, 162, 105248. doi: 10.1016/j.ibiod.2021.105248

Weier, J., & Herring, D. (2000). Measuring vegetation (ndvi & evi). *NASA Earth Observatory*, 20(2).

White, E., & Kaplan, D. (2017). Restore or retreat? Saltwater intrusion and water management in coastal wetlands. *Ecosystem Health and Sustainability*, 3(1), e01258. doi: 10.1002/ehs2.1258

Wong, W. Y., Al-Ani, A. K. I., Hasikin, K., Khairuddin, A. S. M., Razak, S. A., Hizaddin, H. F., ... & Azizan, M. M. (2021). Water, soil and air pollutants' interaction on mangrove ecosystem and corresponding artificial intelligence techniques used in decision support systems-a review. *Ieee Access*, 9, 105532-105563.

Xue, H., Xu, X., Zhu, Q., Yang, G., Long, H., Li, H., ... & Li, Y. (2023). Object-oriented crop classification using time se-ries sentinel images from google earth engine. *Remote Sensing*, 15(5), 1353. doi: 10.3390/rs15051353

Zhao, W., Li, B., Li, R., Wu, X., Lin, G., & Huang, Y. (2024). Urban mangroves at risk: Understanding organophosphate flame retardant pollution at different urban function zones in shenzhen. *Ocean & Coastal Management*, 255, 107262. doi: 0.1016/j.ocecoaman.2024.107262